Deep Bidirectional Classification Model for COVID-19 Disease Infected Patients

Yadunath Pathak, Piyush Kumar Shukla, and K. V. Arya

Abstract—In December of 2019, a novel coronavirus (COVID-19) appeared in Wuhan city, China and has been reported in many countries with millions of people infected within only four months. Chest computed Tomography (CT) has proven to be a useful supplement to reverse transcription polymerase chain reaction (RT-PCR) and has been shown to have high sensitivity to diagnose this condition. Therefore, radiological examinations are becoming crucial in early examination of COVID-19 infection. Currently, CT findings have already been suggested as an important evidence for scientific examination of COVID-19 in Hubei, China. However, classification of patient from chest CT images is not an easy task. Therefore, in this paper, a deep bidirectional long short-term memory network with mixture density network (DBM) model is proposed. To tune the hyperparameters of the DBM model, a Memetic Adaptive Differential Evolution (MADE) algorithm is used. Extensive experiments are drawn by considering the benchmark chest-Computed Tomography (chest-CT) images datasets. Comparative analysis reveals that the proposed MADE-DBM model outperforms the competitive COVID-19 classification approaches in terms of various performance metrics. Therefore, the proposed MADE-DBM model can be used in real-time COVID-19 classification systems.

Index Terms—COVID-19, classification, chest-CT, hyper-parameters

1 Introduction

In December 2019, a severe acute respiratory syndrome coronavirus 2 (SARS-CoV-2) aroused in Wuhan, China and thereafter spread in the whole world [1]. World Health Organization (WHO) named this disease as Coronavirus disease (COVID-19) in February 2020 [2].

The fatality rate depends upon the comorbid medical conditions. The COVID-19 patients with no pre-existing medical conditions have 0.9 percent fatality rate. The imaging such as chest radiography and computed tomography (CT) should be analyzed to detect the severity and treatment of COVID-19 [3], [4]. Chest CT plays an important role in detecting the disease caused by new Corona Virus. National Health Commission of China has motivated the diagnosis based on chest-CT [5]. Chest-CT scan allows for a more detailed view compared to a chest X-ray. For example, a chest X-ray may identify an abnormality, but a chest-CT scan should be able to show the exact location and examine the nature of a formation. Chest x-ray provides a 2D image, while a chest-CT scan is able to produce a 3D view of the organs. An x-ray is built to examine dense tissues, while a CT scan is better able to capture bones, soft tissues and blood vessels simultaneously. Chest x-ray is a good low-cost, first-look examination. However, to move forward with the diagnosis and treatment we might have to capture the chest CT scan achieve detailed information and better image quality.

Bernheim *et al.* [5] have shown that chest CT has limited sensitivity and is a reliable tool to detect COVID-19 disease. The knowledge about the radiological features of COVID-19 patients is unknown and hence, there is an urgent need to develop an automatic standalone tool to test disease through chest-CT of patients.

A large number of approaches such as Random Forest (RF) [6], Support Vector Machine (SVM) [7], Artificial Neural Networks (ANN) [8], [9], Adaptive Neuro-Fuzzy Inference System (ANFIS) [8], [9], and AdaBoost [6] can be used to classify the COVID-19 patients.

However, the aforementioned approaches perform poorly as they require feature selection approaches as a preprocessing tool.

Therefore, Deep Learning (DL) approaches are used to classify COVID-19 patients. The deep learning approaches have the ability to automatically extract the features. Recently many deep learning approaches such as Convolutional Neural Network (CNN) [9], Multi-objective differential evolution based CNN (MCNN) [9], Genetic based CNN (GCNN) [8], CNN and ResNet50 (CNN + ResNet50) [6], AlexNet [6], VGG-16 [6], eXplainable Deep Learning (xDNN) [6], CNN and googlenet (CNN+googlenet) [6], etc. are used to classify COVID-19 patients.

DL approaches can be used to design classification models for COVID-19 disease in patients from the chest-CT images dataset. They can extract the intangible information (i.e., bilateral change) from the chest-CT images and utilize to classify patients as $+ve$ or $-ve$. However, DL approaches

- *Yadunath Pathak is with the Department of Information Technology, Indian Institute of Information Technology (IIIT-Bhopal), Bhopal, Madhya Pradesh 462003, India. E-mail: yadunath@iiitm.ac.in.*
- *Piyush Kumar Shukla is with the Department of Computer Science & Engineering, University Institute of Technology, RGPV, Bhopal, Madhya Pradesh 462033, India. E-mail: piyush@rgtu.net.*
- *K.V. Arya is with the ABV-Indian Institute of Information Technology and Management, Gwalior, Madhya Pradesh 474015, India. E-mail: kvarya@iiitm.ac.in.*

Manuscript received 11 Apr. 2020; revised 30 June 2020; accepted 14 July 2020. Date of publication 20 July 2020; date of current version 6 Aug. 2021. (Corresponding author: Yadunath Pathak.)
Digital Object Identifier no. 10.1109/TCBB.2020.3009859

suffer from overfitting problem due to use of large number of features for classification [10]. Besides the above-mentioned approaches, the classification of COVID-19 patients is still an open research issue.

In this paper, a novel deep learning model is proposed to classify the COVID-19 patients. The major contributions are as follows:

1) Development of deep bidirectional long short-term memory network with mixture density network (DBM) model to classify the COVID-19 patients.
2) An effective use of Memetic Adaptive Differential Evolution (MADE) algorithm to optimize the initial attributes of the DBM model.
3) A multi-objective fitness function is proposed by considering specificity (S_p) and sensitivity (S_n).
4) Extensive experiments are performed by using the COVID-19 datasets of chest-CT images with performance comparison of the proposed model and existing approach for classification of COVID-19 patients.

The remaining paper is organized as: Research motivation and the recent advancements in deep learning-based COVID-19 classification models are presented in Section 2. The mathematical background of the used approaches is discussed in Section 3. The proposed approach is discussed in Section 4. Comparative analyses are performed in Section 5 and finally the paper is concluded in Section 6.

2 Background

The section initially, presents the motivation behind the proposed COVID-19 classification model. Thereafter, the recent advancements in COVID-19 classification models are presented.

2.1 Research motivation

It has been found that the most of COVID-19 infected individuals were identified as having pneumonia and quality CT imaging patterns. Therefore, the radiological examinations are becoming crucial in early examination of COVID-19 infection. Currently, CT findings have already been suggested as an important evidence for scientific examination of COVID-19 in Hubei, China. However, classification of patient from chest CT images is not an easy task. Therefore, in this paper, a COVID-19 infected patients classification model is proposed.

However, the existing classification models such as histogram of oriented gradients (HOG) use hand crafted features, and the classifier like SVM cannot backpropagate the error to the input which pose hindrance as well affect the accuracy in automated classification system. To address the above issues in the resent research, a deep bidirectional long short-term memory network with mixture density network (DBM) is used in this paper [11]. The DBM comes up with more number of hidden layers, accordingly it can work as a feature extraction and prediction model, which will be end-to-end trainable. The hidden layers of the DBM are made up of a bank of filters whose weights are learned during the training process. These are used for automatic feature extraction.

The other layers in the DBM are employed to optimize the number of parameters and the size of the feature descriptor while still retaining most, of the useful information from the input dataset in the form of feature descriptors. The probability likelihood maximization is employed to fine-tuning of feature descriptor indirectly. To obtain the better performance of the DBM. Also, the DBM model generates a multi-modal distribution of outputs. Therefore, it can present the arbitrary conditional probability distributions of detailed output variables.

From the literature review, it was observed that the hyperparameters tuning issue associated with deep learning models is neglected by the majority of the researchers. Therefore, the memetic adaptive differential evolution (MADE) algorithm has been used to tune the hyperparameters of bidirectional long short-term memory network with mixture density network.

2.2 Related Work

Recently, researchers have perceived the imaging patterns on chest-CT for detecting the COVID-19 [4], [5]. Fang *et al.* [12] analyzed the results obtained from chest-CT and Reverse transcription-polymerase chain reaction (RT-PCR) and reported that detection rate of CT (98 percent) is much higher than RT-PCR (71 percent). Das *et al.* [4] studied chest-CT of twenty-one infected patients and observed that the lung abnormalities in chest-CT shows the severity of disease after the onset of the initial symptoms. Xie *et al.* [13] after analyzing the chest-CT of 167 patients found that single chest-CT and the combination of chest-CT and RT-PCR provides better detection rate than RT-PCR alone. Chuang *et al.* [14] investigated chest-CTs of 21 COVID-19 infected patients and detected the high concentration of ground-glass opacities and peripheral lung distribution. Song *et al.* [15] found that greater consolidation in chest-CT reveals the evolution of the disease. Zu *et al.* [16] reviewed the chest-CT imaging features of COVID-19 that may help to detect the disease in an early stage. NG *et al.* [17] studied chest radiographs of twenty-one patients in Shenzhen and Hong Kong, China and confirmed the finding of bilateral and peripheral ground-glass with or without consolidation in the lung. Chen *et al.* [18] studied chest-CT of 99 patients and found the bilateral pneumonia was the most common verdict in the chest. Lei *et al.* [19] studies the chest-CT for diagnosis of the infected patient where the observation report in some case revealed that smaller size and absorption of these lesions indicated the improvement in patients [20], [21]. Based on the above-mentioned facts, it is observed that the automatic prediction framework is required for early detection of COVID-19 patients using chest-CT.

An eXplainable Deep Learning (xDNN) model to test COVID-19 disease in patients was implemented by Soares *et al.* [6]. It has achieved remarkable performance as compared to the existing models.

Singh *et al.* designed a multi-objective differential evolution-based convolutional neural networks (MCNN) to classify chest-CT images in three classes such as COVID-19 (+), COVID-19 (-), and pneumonia patients [9].

From the extensive review, it has been found that the researchers have neglected the use of a computational model for COVID-19's classification. Therefore, the machine and deep learning models can be utilized to classify COVID-19 patients from chest-CT images. In this paper, initially, the

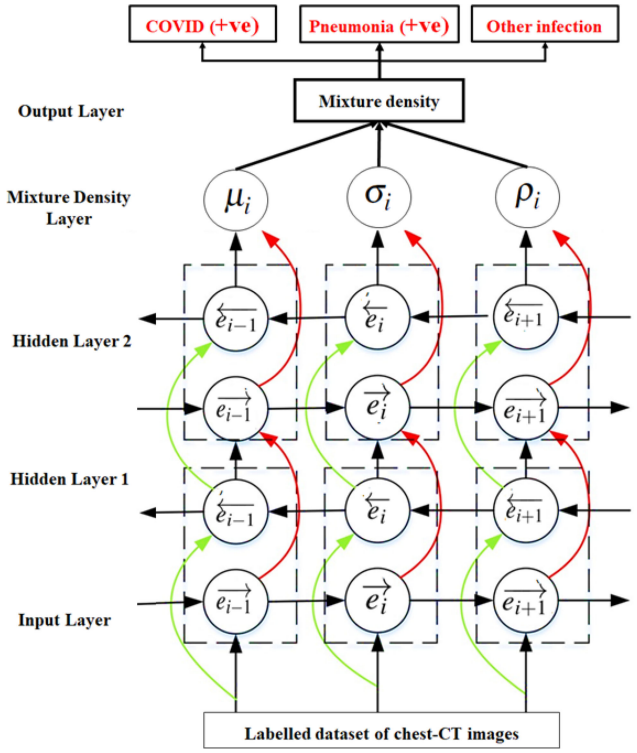

Fig. 1. Deep bidirectional long short-term memory network with mixture density network (DBM) based COVID-19 disease classification.

DBM model is proposed to classify COVID-19 disease in patients. Thereafter, MADE algorithm is used to tune the initial parameters of the DBM model.

3 Mathematical Preliminaries

To understand the proposed computational model the required mathematical background is presented here for all the three building blocks of the proposed framework.

3.1 Deep Bidirectional Long Short-Term Memory Network With Mixture Density Network

The diagrammatic flow of the DBM model is shown in Fig. 1. DBM contains two hidden layers and the output layer contains three weighted Mixture Density Networks (MDNs). The horizontal edges demonstrate bidirectional flow in the temporal axis. The vertical edges provide the one-way flow between hidden and input layers and also between input and hidden layers. Green and red edges show forward and backward unit flows, respectively.

Assume that $H = \{(o^f, u^f)\}_{f=1}^{M}$ shows group of M features. For feature f, an input u^f contain four features like a trajectory in three directions and time clock but, an output o^f is influenced by several tasks.

Long Short-Term Memory (LSTM) uses three gates to handle of vanishing of gradient problem. An input gate (G_i) can be represented as

$$G_i = \sigma(\varphi_{uG} u_i + \varphi_{qG} q_{i-1} + c_G). \tag{1}$$

A forget gate (R_i) at i is represented as

$$R_i = \sigma(\varphi_{uR} u_i + \varphi_{qR} q_{i-1} + c_R). \tag{2}$$

An output gate (P_i) at i can be described as

$$P_i = \sigma(\varphi_{uP} u_i + \varphi_{qP} q_{i-1} + c_P). \tag{3}$$

An internal memory (e_i) at i can be described as

$$e_i = R_i \circledast e_{i-1} + G_i \circledast tanh(\varphi_{qe} q_{i-1} + \varphi_{ue} u_i + c_e). \tag{4}$$

LSTM output (q_i) at i can be described as

$$q_i = P_i \circledast tanh(e_i), \tag{5}$$

where $\circledast$ represents an element-wise multiplication, $\sigma(\bullet)$ shows a sigmoid activation function, and $LSTM(\bullet)$ is used to represent all functions of LSTM from Eqs. (1) to (5). Therefore, a single binary LSTM layer can be integrated with a forward and backward sequences

$$\left.\begin{array}{ll} \overrightarrow{e_i} & = LSTM(u_i, \overrightarrow{e_{i-1}}) \\ \overleftarrow{e_i} & = LSTM(u_i, \overleftarrow{e_{i+1}}) \\ o_i & = a(\varphi_{\overrightarrow{eo}} \overleftarrow{e_i} + \varphi_{\overleftarrow{eo}} \overleftarrow{e_i} + c_o) \end{array}\right\}, \tag{6}$$

where φ_{ts} defines a weight from t to s, $a(\bullet)$ shows the activation function, c_s represents bias at layer s, and for activation function the Rectified Linear Unit (ReLU) [22] has been used.

Gaussian function $(M(\bullet))$ is utilized as PDF for output layer as

$$F(o_i|M_i) = \sum_{j=1}^{J} \omega_i^j M(o_i|\rho_i^j, \sigma_i^j, \mu_i^j), \tag{7}$$

where J represents number of PDFs, o_i defines actual values, and ω_i^j shows the coefficient of Jth PDF.

The attributes in $M(\bullet)$ can be evaluated as

$$\begin{aligned} \rho_i^j &= tanh(\tilde{\rho}_i^j) \\ \sigma_i^j &= exp(\tilde{\sigma}_i^j) \\ \omega_i^j &= \frac{exp(\tilde{\omega}_i^j)}{\sum_{j=1}^{J} exp(\tilde{\omega}_i^j)} \\ \mu_i^j &= \tilde{\mu}_i^j, \end{aligned} \tag{8}$$

where $\tilde{\sigma}_i^j$ and $\tilde{\mu}_i^j$ define a variance and an average of the output layer, respectively. $\tilde{\omega}_i^j$ and $\tilde{\rho}_i^j$ define coefficient of PDF and correlation of jth Gaussian component, respectively.

The probability likelihood function is defined to obtain efficient classification results. It can be evaluated as

$$L(x) = \sum_{i=1}^{Z} -log\left(\sum_{j=1}^{J} \omega_i^j M(o_i|\rho_i^c, \sigma_i^c, \mu_i^c)\right), \tag{9}$$

where Z defines a number of features. To minimize the loss function, MADE algorithm is utilized.

3.2 Memetic Differential Evolution

Jia *et al.* [23] proposed a memetic differential evolution (MDE) to obtain optimal solutions to many complex engineering problems. Unlike standard differential evolution, MDE has an ability to adaptively controls the scaling factor (F) and crossover Rate (CR) operators. Thus, MDE can efficiently

balance between population diversity and fast convergence speed. Additionally, it overcomes the stuck in local optima issue with differential evolution by using a chaotic local search. MDE is defined into the following steps:

1. *Initialization:* Initially, MDE is originated by defining various parameters like population size (N_p), mutation rate (R_m), and crossover rate (R_c). Initial individuals such as $\tau_\iota^0(\iota = 1, 2, \ldots, N_p)$ are obtained randomly. The evolution process is monitored by using ($h = 0$) and maximum number of allowed iterations (h_M).
2. *Evolution phase:* Crossover and mutation operations are utilized to enhance the convergence speed.
   i. *Mutation:* Mutation is applied on solution vector τ_ι^h to compute a new solution vector Π_ι^h. There are many mutation operators some of them are described as

$$\Pi_\iota^h = \tau_{d1}^h + R_m.(\tau_{d2}^h - \tau_{d3}^h), \tag{10}$$

   where d_1, d_2, and d_3 are randomly values obtained from $[1,\ N_p,]$. ι defines index values. $d_i \neq \iota\ \forall i = 1:3$.
   ii. *Crossover:* In crossover, $\forall\ \tau_\iota^h$, a child solution χ_ι^h is computed as

$$\chi_{\iota_\eta}^h = \begin{cases} \Pi_{\iota_\eta}^h, & \beta_\eta \leq R_c \quad \text{or} \quad \eta = \eta_{d_n}\ \eta \\ \tau_{\iota_\eta}^h, & otherwise \end{cases} = 1, 2, \ldots, D, \tag{11}$$

   where $\beta_\eta \in [0,\ 1]$ and $\eta_{d_n} \in [1,\ D]$. Here, D denotes the number of dimensions used in optimization problem.
3. *Selection:* A child solution (χ_ι^h) is defined along with its parent solution (τ_ι^h) as

$$\tau_\iota^{h+1} = \begin{cases} \chi_\iota^h, & f(\chi_\iota^h) \leq f(\tau_\iota^h) \\ \tau_\iota^h, & otherwise \end{cases}. \tag{12}$$

4. *Chaotic local search:* Local search is utilized on the best-evaluated solution by considering the chaotic system to obtain new solutions. It improves the local search ability of the differential evolution and overcomes the problem of stuck in local optima issue.
5. *Termination criteria:* Till termination criteria not satisfied, Steps 2 and 3 will be repeated.

4 Proposed COVID-19 Classification Model

In this section, the hyperparameters tuning issue with DBM is overcome by using the Memetic Adaptive Differential Evolution (MADE) algorithm.

4.1 Problem Statement

Like other existing classification approaches the proposed COVID-19 classification approach also has the challenges associated with the hyperparameters tuning. Table 1 depicts number of initial parameters required by the proposed COVID-19 classification approach along with their respective data type, lower and upper limits, and constraints.

TABLE 1
Hyper-Parameters of the Proposed COVID-19 Classification Approach

Parameter	Lower bound	Upper bound	Data type
Number of layers	3	9	Integer
Number of nodes	40	200	Integer
Clip Gradients	2	10	Integer
Batch Size	2	100	Integer
Learning Rate	0	1	Float
Epochs	100	1000	Integer

Manual tuning of these attributes may reduce the performance of the proposed COVID-19 classification approach. Also, manual tuning is a time-consuming process.

4.2 Multi-Objective Fitness Function

A multi-objective fitness function ($f(t)$) is defined for initial parameters selection of the proposed COVID-19 classification approach. The performance metrics, i.e., sensitivity (S_n) and specificity (S_p) are utilized to define $f(t)$ as

$$f(t) = \begin{cases} Maximize\ (S_n) \\ Maximize\ (S_p) \end{cases}. \tag{13}$$

Here, S_n is defined as

$$S_n = \frac{T_p}{T_p\ +\ F_n}. \tag{14}$$

Here, T_p, T_n, F_p, and F_n represent true positive, true negative, false positive, and false negative respectively. Positive represents those patients who suffer from COVID-19 disease. Negative represents those patients who suffer from pneumonia or some other kinds of lung diseases.

S_p can be computed as

$$S_p = \frac{T_n}{T_n\ +\ F_p}. \tag{15}$$

4.3 Memetic Adaptive Differential Evolution

From the literature, it has been found that MDE is sensitive to crossover and mutation operators. To overcome this issue, Liao *et al.* [24] designed MADE algorithm to optimize engineering problems in a more efficient manner [25]. The MADE based proposed COVID-19 classification approach is demonstrated in Fig. 2. The step-wise description of proposed model is given below:

Step 1. Initialization. In this step, the initial population S_1^0 ($S_1^0\ \in N_p$) is generated and the control parameters such as R_m, R_c, and B_g = 0.6 are initiated. Initially, generation start from 0, i.e., $h = 0$. Let $S_2^0 = S_1^0$.

Step 2. Evolution. In this step, the population is evolved by utilizing mutation and crossover operations.

i. *Mutation:* The trial vector (Π_ι^h) can be generated for every $\tau_\iota^h(\iota = 1, 2, \ldots, N_p)$ by using the following mutation operation:

$$\Pi_\iota^h = \tau_{d1}^h + R_m.(\tau_{archive,\iota}^h - \tau_{d2}^h), \tag{16}$$

where $\tau_{archive,\iota}^h$ is selected randomly from S_2^h.

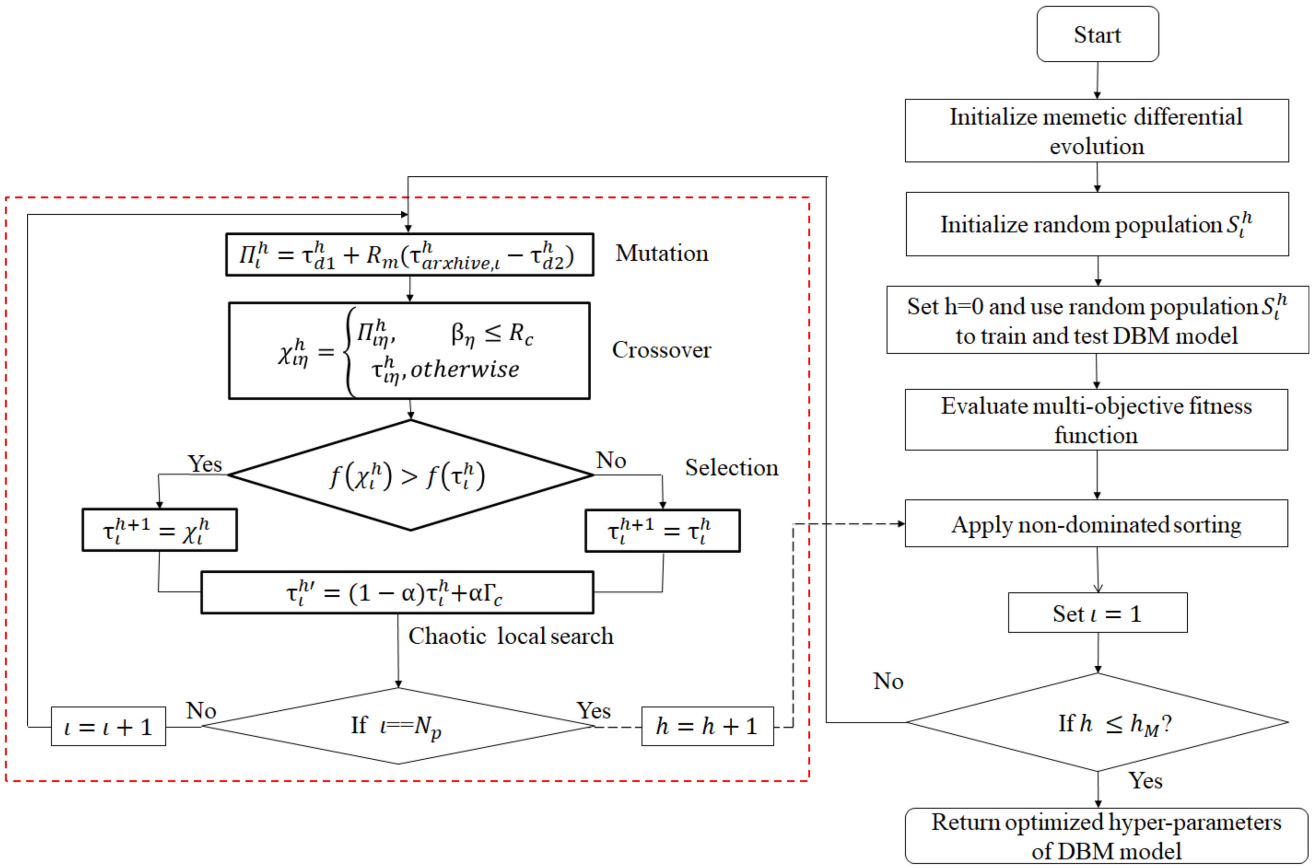

Fig. 2. Flowchart of the proposed MADE-DBM model for COVID-19 classification.

ii. *Boundary evaluation:* If $d_n > B_g$, then

$$\Pi_{\iota_\eta}^h = \begin{cases} \tau_{d\eta}^h \Pi_{\iota_\eta} < L_b \\ \tau_{d\eta}^h \Pi_{\iota_\eta} > U_b \end{cases}'$$

otherwise, non-feasible parameters are redefined randomly from feasible region $\lambda \in [L_b, U_b]$.

where L_b and U_b are lower and upper limits of ιth vector. $d_n \in [0, 1]$.

iii. *Crossover:* A child solution χ_ι^h can be evaluated by using Eq. (11).

Step 3. Selection. Selection operator can be implemented as:

1) If $\tau_\iota^h > \chi_\iota^h$, then τ_ι^h is placed in S_1^h.
2) If $\chi_\iota^h > \tau_\iota^h$, then τ_ι^h is replaced by χ_ι^h in S_1^h.
3) If τ_ι^h and χ_ι^h are not dominated solutions, then χ_ι^h is also considered in S_1^h .

Step 4. Sorting of individuals. N_p solution vectors are selected from S_1^h using Non-dominated sorting [26] and crowding distance sorting. Then, these solutions are stored at S_2^h population. It will improve the population diversity.

Step 5. Chaotic local search. The obtained best solution, i.e., τ_ι^h is further improved by using the chaotic linear search (CLS). It can be defined as

$$\tau_\iota^{h'} = (1-\alpha)\tau_\iota^h + \alpha\Gamma_c. \tag{17}$$

Here, $\tau_\iota^{h'}$ defines new child vectors of τ_ι^h obtained from chaotic linear search. α defines the shrinking scale and can be evaluated as

$$\alpha = 1 - \left| \frac{FEs - 1}{FEs} \right|^\kappa, \tag{18}$$

where FEs represents the number of function evaluations, and κ is used to monitors the shrinking speed. If κ contains low value, then shrinking speed should be high.

Γ_c can be evaluated as

$$\Gamma_c = U + \Gamma_i^\nu \cdot (V - U). \tag{19}$$

Here, $[U, V]$ defines the search space of τ_ι. Γ_i^ν is evaluated by using the chaotic logistic map and can be defined as

$$\Gamma_i^{\nu+1} = \mu\Gamma_i^\nu(1 - \Gamma_i^\nu), \nu = 1, 2, \ldots; \Gamma_i \in [0, 1]. \tag{20}$$

Here, Γ_i^ν defines the ith chaotic attribute in νth iteration. μ defines the bifurcation control parameter. Also, $\Gamma_i \neq 0.25$, 0.5, and 0.75.

Step 6. Set $h = h + 1$

Step 7. Repeat steps 2 to 6 till $h \leq h_M$.

5 Performance Analysis

The proposed MADE-DBM model is implemented on benchmark datasets of chest-CT images. Some well-known COVID-19 classification approaches such as Support Vector Machine (SVM) [7], Random Forest (RF) [6], Artificial Neural Networks (ANN) [8], [9], Adaptive Neuro-Fuzzy Inference System (ANFIS) [8], [9], Convolutional Neural Network (CNN) [9], Multi-objective differential evolution based CNN (MCNN) [9], Genetic based CNN (GCNN) [8],

TABLE 2
Hyper-Parameters of Memetic Adaptive Differential Evolution (MADE) Algorithm

Attribute	Value
Population size	60
Selection	Tournament
Mutation ratio	0.01
Population type	Double vector
Crossover ratio	0.2
Stopping criteria	Generations: 500

CNN and ResNet50 (CNN + ResNet50) [6], AdaBoost [6], AlexNet [6], VGG-16 [6], xDNN [6], and CNN and googlenet (CNN+googlenet) [6] are considered for comparative analyses. 20-fold cross-validation is also utilized to overcome the overfitting issue. The proposed COVID-19 classification model is implemented on Intel(R) Core(TM) $i7$ 3.60 GHz with 32-GB RAM on MATLAB $2018b$ software. Initial parameters of the proposed MADE-DBM model are selected by using MADE. The hyperparameters of MADE are shown in Table 2.

5.1 Comparative Analysis on Binary Dataset

Soares *et al.* observed imaging patterns on chest-CT images (both inspiratory and expiratory) of COVID-19 disease in patients. The chest-CT images of the intensive care unit (ICU) patients on admission constitute the typical discoveries by showing sub-segmental areas of consolidation and bilateral multiple lobular while those of non-ICU patients consist of sub-segmental areas of consolidation and bilateral ground-glass opacity. Wu *et al.* [27] observed that at later stage the chest-CT images of these patients display bilateral ground-glass opacity with resolved consolidation. Therefore, in this work also the chest-CT images are being used for classification of the COVID-19 patients.

For experimental purpose, Soares *et al.* provided a SARS-CoV-2 CT scan dataset [6]. This dataset contains 1,252 CT scan images of 60 (32 male $+28$ female) COVID-19 infected patients and 1,230 CT scan images of 60 normal patients (30 male $+30$ female). Therefore, in total 2,482 CT scan images are available for experimental purpose from the patients in hospitals of Sao Paulo, Brazil [6]. Fig. 3 shows the samples of chest-CT scans of COVID-19 infected patients.

We have utilized the "median $\pm$ $IQR \times 1.5$" values of the computed results when we have trained and tested the proposed and the competitive models on different fractions of the training and testing ratio as 60 and 40 percent, respectively.

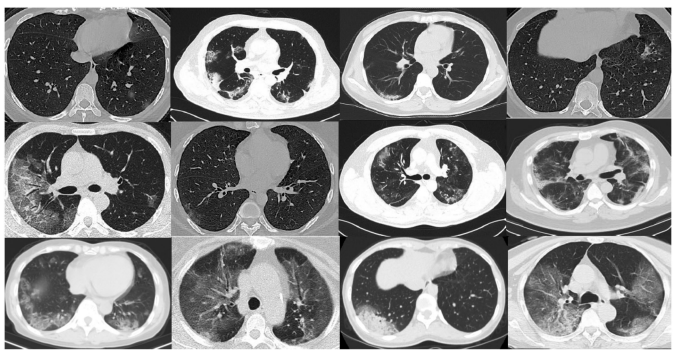

Fig. 3. A view of chest-CT scan images of COVID-19 disease in patients.

TABLE 3
Performance Analyses of the Proposed COVID-19 Diagnostic Testing Model on Binary Class Dataset by Utilizing Confusion Matrix Based Performance Metrics When Training to Testing Ratio is 60:40

Models	Accuracy	F-measure	Recall	Precision	AUC
SVM	91.81%	91.76%	91.92%	92.38%	91.37%
RF	93.49%	93.21%	95.83%	94.82%	93.72%
AdaBoost	95.16%	95.14%	96.71%	93.63%	95.19%
AlexNet	93.75%	93.61%	92.28%	94.98%	93.68%
VGG-16	94.96%	94.97%	95.43%	94.02%	94.96%
GoogleNet	91.73%	91.82%	93.50%	90.20%	91.79%
ResNet	94.96%	95.03%	97.15%	93.00%	94.98%
xDNN	97.38%	97.31%	95.53%	99.16%	97.36%
DBM	97.23%	97.89%	97.68%	98.14%	97.71%
Proposed	98.37%	98.14%	98.87%	98.74%	98.32%

Table 3 depicts comparative analyses among the proposed and the competitive models in terms of accuracy, f-measure, recall, precision, and area under curve (AUC). It shows that the proposed model provides significantly good performance as compared to the existing models. It is found that the proposed model not only achieves significant accuracy, but it also achieves significant AUC value. Therefore, the proposed model can be used for real-time testing of COVID-19 patients.

5.2 The Performance Analysis on a Three-Class COVID-19 Chest-CT Dataset

We have also obtained chest-CT dataset from Singh *et al.* [9] with three classes such as COVID-19 (+), COVID-19 (-), and pneumonia patients. It contains 1,790 chest-CT images of 80 patients. Out of these 612 chest-CT images have been obtained from 27 COVID-19 infected patients. 631 images have been obtained from 30 pneumonia infected patients. Remaining 547 images have been obtained from 23 patients either infected from some other diseases or not infected from any disease.

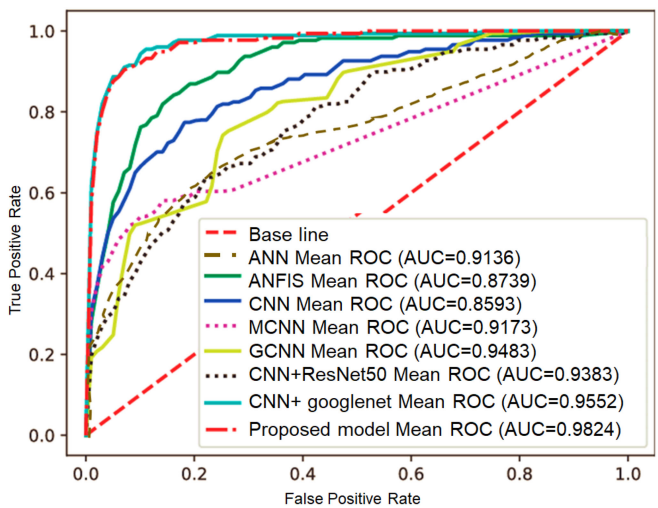

Fig. 4. Area under curve analysis of the proposed diagnostic testing model (True positive rate versus False positive rate).

TABLE 4
Training Analyses of the Proposed COVID-19 Diagnostic Testing Model on Three Class COVID-19 Chest-CT by Utilizing Confusion Matrix Based Performance Metrics When Training to Testing Ratio is 60:40

Model	AUC	F-measure	Sensitivity	Specificity	Accuracy
ANN	0.885246	0.861234	0.865385	0.880546	0.872727
ANFIS	0.908197	0.896667	0.899351	0.905724	0.902479
CNN	0.921311	0.956667	0.955782	0.922832	0.938843
MCNN	0.937705	0.923333	0.925566	0.935811	0.930579
GCNN	0.947541	0.984343	0.979661	0.948387	0.963636
CNN+ResNet50	0.957377	0.976667	0.976589	0.957516	0.966942
CNN+googlenet	0.965574	0.968333	0.968751	0.965116	0.966942
Proposed	0.977049	0.981667	0.981878	0.976783	0.979339

TABLE 5
Testing (i.e., Validation) Analyses of the Proposed COVID-19 Diagnostic Testing Model on Three Class COVID-19 Chest-CT Dataset by Utilizing Confusion Matrix Based Performance Metrics When Training to Testing Ratio is 60:40

Model	AUC	F-measure	Sensitivity	Specificity	Accuracy
ANN	0.886885	0.856667	0.862839	0.881647	0.871901
ANFIS	0.895082	0.876667	0.880645	0.891525	0.885952
CNN	0.908197	0.936667	0.935811	0.909385	0.922314
MCNN	0.919672	0.905766	0.907767	0.917232	0.912397
GCNN	0.934426	0.961356	0.959596	0.935065	0.947107
CNN+ResNet50	0.937705	0.956667	0.956522	0.937908	0.947107
CNN+googlenet	0.949182	0.942146	0.941463	0.947899	0.944628
Proposed	0.962295	0.961667	0.962295	0.961667	0.961983

Various classification measures are utilized to compute the effectiveness of the proposed diagnostic testing model over the existing models. These metrics are F-measure, accuracy, area under curve (AUC), sensitivity, and specificity.

The AUC i.e., true positive rate versus false positive rate of the proposed diagnostic testing model is shown in Fig. 4. It is found that the proposed diagnostic testing model achieves significantly higher AUC value as compared to other models. It also indicates that the proposed diagnostic testing model can efficiently diagnose COVID-19 disease in patients.

Tables 4 and 5 shows the training and validation analysis of the proposed COVID-19 diagnostic testing model. Performance metrics such as accuracy, AUC, f-measure, specificity, and sensitivity are considered to evaluate the performance of the designed COVID-19 diagnostic testing model. From these tables, it is evident that the proposed diagnostic testing model outperformed the competitive models. Thus, the proposed MADE-DBM testing model poses itself as a technological alternative to COVID-19 testing tools.

6 Conclusion

A novel MADE based DBM model is proposed to classify the COVID-19 patients. Multi-objective fitness function has been designed using sensitivity (S_n) and specificity (S_p). The proposed model has been made automatic, and the hyperparameters of the DMB model have been tuned and optimized using MADE algorithm. Thereafter, the proposed MADE-DBM model has been validated on two different benchmark COVID-19 datasets of chest-CT images. To prevent the MADE-DBM model from overfitting issue, 20-fold validation was also utilized. The performance analysis on both the benchmark chest-CT databases revealed that the proposed MADE-DBM model outperformed the competitive models in terms of various performance metrics such as accuracy, area under curve (AUC), f-measure, sensitivity, specificity, recall and precision by 1.7912, 1.5256, 1.8372, 1.9272, 0.4382, 1.6382, and 1.5256 percent, respectively. Therefore, the proposed MADE-DBM model can be utilized for real-time testing of the COVID-19 disease in patients.

References

[1] H. Y. F. Wong *et al.*, "Frequency and distribution of chest radiographic findings in COVID-19 positive patients," *Radiology*, vol. 296, no. 2, 2020, Art. no. 201160.

[2] J. P. Kanne, "Chest CT findings in 2019 Novel Coronavirus (2019-nCoV) infections from Wuhan, China: Key points for the radiologist," *Radiology*, vol. 295, pp. 16–17, 2020.

[3] C. W. Lam, M. H. Chan, and C. K. Wong, "Severe acute respiratory syndrome: Clinical and laboratory manifestations," *Clin. Biochemist Rev.*, vol. 25, no. 2, 2004, Art. no. 121.

[4] N. N. Das, N. Kumar, M. Kaur, V. Kumar, and D. Singh, "Automated deep transfer learning-based approach for detection of COVID-19 infection in chest X-rays," *Innov. Res. BioMed.*, 2020, doi: 10.1016/j.irbm.2020.07.001.

[5] A. Jaiswal, N. Gianchandani, D. Singh, V. Kumar, and M. Kaur, "Classification of the COVID-19 infected patients using DenseNet201 based deep transfer learning," *J. Biomol. Struct. Dyn.*, pp. 1–8, 2020. [Online]. Available: https://doi.org/10.1080/07391102.2020.1788642

[6] E. Soares, P. Angelov, S. Biaso, M. H. Froes, and D. K. Abe, "SARS-CoC-2 CT-scan dataset: A large dataset of real patients CT scans for SARS-CoV-2 identification," *medRxiv*, 2020. [Online]. Available: https://doi.org/10.1101/2020.04.24.20078584

[7] G. Qi, H. Wang, M. Haner, C. Weng, S. Chen, and Z. Zhu, "Convolutional neural network based detection and judgement of environmental obstacle in vehicle operation," *CAAI Trans. Intell. Technol.*, vol. 4, no. 2, pp. 80–91, 2019.

[8] Y. Pathak, P. K. Shukla, A. Tiwari, S. Stalin, S. Singh, and P. K. Shukla, "Deep transfer learning based classification model for COVID-19 disease," *Innov. Res. BioMed.*, 2020, doi: 10.1016/j.irbm.2020.05.003.
[9] D. Singh, V. Kumar, Vaishali, and M. Kaur, "Classification of COVID-19 patients from chest CT images using multi-objective differential evolution–based convolutional neural networks," *Eur. J. Clin. Microbiol. Infect. Dis.*, vol. 39, pp. 1379–1389, 2020.
[10] Y. Tingting, W. Junqian, W. Lintai, and X. Yong, "Three-stage network for age estimation," *CAAI Trans. Intell. Technol.*, vol. 4, no. 2, pp. 122–126, 2019.
[11] Y. Zhao, R. Yang, G. Chevalier, R. C. Shah, and R. Romijnders, "Applying deep bidirectional LSTM and mixture density network for basketball trajectory prediction," *Optik*, vol. 158, pp. 266–272, 2018.
[12] Y. Fang, H. Zhang, Y. Xu, J. Xie, P. Pang, and W. Ji, "CT manifestations of two cases of 2019 novel Coronavirus (2019-nCoV) Pneumonia," *Radiology*, vol. 295, 2020, Art. no. 200280.
[13] X. Xie, Z. Zhong, W. Zhao, C. Zheng, F. Wang, and J. Liu, "Chest CT for typical 2019-nCoV Pneumonia: Relationship to negative RT-PCR testing," *Radiology*, vol. 296, no. 2, 2020, Art. no. 200343.
[14] M. Chung *et al.*, "CT imaging features of 2019 Novel Coronavirus (2019-nCoV)," *Radiology*, vol. 295, no. 1, pp. 202–207, 2020.
[15] F. Song *et al.*, "Emerging 2019 Novel Coronavirus (2019-nCoV) Pneumonia," *Radiology*, vol. 295, 2020, Art. no. 200274.
[16] Z. Y. Zu *et al.*, "Coronavirus disease 2019 (COVID-19): A perspective from China," *Radiology*, vol. 296, no. 2, 2020, Art. no. 200490.
[17] M.-Y. Ng *et al.*, "Imaging profile of the COVID-19 infection: Radiologic findings and literature review," *Radiol.: Cardiothoracic Imag.*, vol. 2, no. 1, 2020, Art. no. e200034.
[18] T. Liu *et al.*, "Spectrum of chest CT findings in a familial cluster of COVID-19 infection," *Radiol.: Cardiothoracic Imag.*, vol. 2, no. 1, 2020, Art. no. e200025.
[19] J. Lei, J. Li, X. Li, and X. Qi, "CT imaging of the 2019 Novel Coronavirus (2019-nCoV) Pneumonia," *Radiology*, vol. 295, no. 1, pp. 18–18, 2020.
[20] H. S. Basavegowda and G. Dagnew, "Deep learning approach for microarray cancer data classification," *CAAI Trans. Intell. Technol.*, vol. 5, no. 1, pp. 22–33, 2020.
[21] Y. Wu, Y.-L. Xie, and X. Wang, "Longitudinal CT findings in COVID-19 Pneumonia: Case presenting organizing pneumonia pattern," *Radiol.: Cardiothoracic Imag.*, vol. 2, no. 1, 2020, Art. no. e200031.
[22] D. Yarotsky, "Error bounds for approximations with deep ReLU networks," *Neural Netw.*, vol. 94, pp. 103–114, 2017.
[23] D. Jia, G. Zheng, and M. K. Khan, "An effective memetic differential evolution algorithm based on chaotic local search," *Inf. Sci.*, vol. 181, no. 15, pp. 3175–3187, 2011.
[24] Q. Liao, Q.-Q. Fan, and J.-J. Li, "Translation control of an immersed tunnel element using a multi-objective differential evolution algorithm," *Comput. Ind. Eng.*, vol. 130, pp. 158–165, 2019.
[25] Q. Fan and X. Yan, "Multi-objective modified differential evolution algorithm with archive-base mutation for solving multi-objective xylene oxidation rocess," *J. Intell. Manuf.*, vol. 29, no. 1, pp. 35–49, 2018.
[26] K. Deb, S. Agrawal, A. Pratap, and T. Meyarivan, "A fast elitist non-dominated sorting genetic algorithm for multi-objective optimization: NSGA-II," in *Proc. Int. Conf. Parallel Problem Solving Nat.*, 2000, pp. 849–858.
[27] Y. Wu, Y.-L. Xie, and X. Wang, "Longitudinal CT findings in COVID-19 Pneumonia: Case presenting organizing pneumonia pattern," *Radiol.: Cardiothoracic Imag.*, vol. 2, no. 1, 2020, Art. no. e200031.

Yadunath Pathak received the PhD degree from the Computer Science and Engineering Department, Atal Bihari Vajpayee Indian Institute of Information Technology and Management (ABV-IIITM), Gwalior, Madhya Pradesh, India. He is currently working as assistant professor with the Indian Institute of Information Technology (IIIT), Bhopal. He is having more than six year of teaching and research experience. His research interests include bio-medical engineering, digital image processing, and machine learning techniques. He has to his credit three Indian patents (Published) and more than 10 publications in reputed SCI-Indexed Journals and International Conferences.

Piyush Kumar Shukla received the BE degree in EC from LNCT-Bhopal, Madhya Pradesh, India, the MTech degree in CSE from SATI, Vidisha, Madhya Pradesh, India, and the PhD degree in computer science and engineering from the Department of CSE, UIT, RGPV, Bhopal, Madhya Pradesh, India. He is working as an associate professor with the Department of Computer Science and Engineering, UIT-RGP (Technological University of Madhya Pradesh), Bhopal, Madhya Pradesh, India. He is having around 15 Years of Experience in teaching and research. He has completed Post Doctorate Fellowship(PDF) tilted "White Box Cryptography for Smart and Intelligent Devices" recently under "Information Security Education and Awareness Project Phase II" funded by Ministry of Electronics and Information Technology (MeitY), from SVNIT Surat, Gujarat, India. His research interests include white-box cryptography, information security and privacy, cyber security, dynamic wireless network, machine learning, Internet of Things, image processing, blockchain, and IoT. He has published three books with the international publisher, published more than 10 book chapters in International publishers, i.e., IGI-Global, Springer, and Elsevier books, 04 Books under publication with Taylor and Francis, Apple Academic Publisher, Scrivener, and Wiley. He has published more than 15 Indian Patents, 13 SCIE/SCI Indexing Journal papers, 50 publications in SCOPUS Journals including Chapters in International Books or International Conferences. Completed and got Certificate of NPTEL Twelve Week Course in cryptography and network security, computer networks and Internet protocols, digital circuits, signals and systems, computer architecture course with Elite.

K. V. Arya received the BSc degree from Rohilkhand University, Bareilly, India, the ME (Integrated) degree from the Indian Institute of Science, Bangalore, India, and the PhD degree in computer science and engineering from the Indian Institute of Technology Kanpur, Kanpur, India. He has been an professor with the Department of Computer Science and Engineering, Atal Bihari Vajpayee Indian Institute of Information Technology and Management, Gwalior, Madhya Pradesh, India. He has more than 25 years of teaching and research experience. He has more than 120 research papers in international journals, book chapters, and conference proceedings. His main research focuses on image processing: Image enhancement, image registration, biometrics: Face recognition, Iris recognition, gait, wireless ad hoc networks: Energy aware routing, secure routing, and information security: Intrusion detection and prevention.